arXiv:0912.2024v1 [physics.optics] 10 Dec 2009

Nanorod optical antennas for dipolar transitions

Tim H. Taminiau[1],* Fernando D. Stefani[2], and Niek F. van Hulst[1†]

[1] *ICFO-Institut de Ciencies Fotoniques,*

Mediterranean Technology Park, 08860 Castelldefels (Barcelona), Spain.

[2] *Photonics and Optoelectronics Group,*

Ludwig-Maximilians-Universität München and CeNS,

Amalienstrasse 54, 80799 Munich, Germany.

(Dated: February 4, 2022)

Abstract

Optical antennas link objects to light. Here, we analyze metal nanorod antennas as cavities with variable reflection coefficients to derive the interaction of dipolar transitions with radiation through the antenna modes. The presented analytical model accurately describes the complete emission process, and is summarized in a phase-matching equation. We show how antenna modes evolve as they become increasingly more bound, i.e. plasmonic. The results illustrate why efficient antennas should not be too plasmonic, and how subradiant even modes can evolve into weakly-interacting dark modes. Our description is valid for the interaction of nanorods with light in general, and is thus widely applicable.

*Electronic address: Tim.Taminiau@icfo.es

†ICREA - Institució Catalana de Recerca i Estudis Avançats, Spain.

Optical antennas improve the interaction of an object with optical radiation by means of a near-field coupling. The object absorbs and emits light through the antenna modes [1, 2]. Metallic nano-particles are especially suited as optical antennas because they support confined plasmon modes that respond strongly to light [3, 4]. With optical antennas, the electronic transitions of quantum emitters, such as molecules and quantum dots, can be controlled. Excitation and emission rates are enhanced [5, 6, 7], the spectral dependence shaped [8], and the angular emission directed [2, 9].

To understand optical antennas, and how they differ from conventional antennas, the Mie solutions are available for ellipsoids [8], and extensive numerical studies are performed for other shapes [10]. More intuitively, antennas have been described as resonators or (Fabry-Pérot) cavities [1, 11, 12, 13, 14, 15, 16, 17]. If the wave vector in/along the cavity is known, the position of the resonant modes can be determined [18, 19]. However, the functionality of an antenna is not given by the value of the resonance length or wavelength alone, but by how its modes interact with a local object and with radiation.

In this letter, we derive the interaction of dipolar transitions with radiation through optical antenna modes by treating the antenna as a cavity resonator. The obtained analytical model accurately describes the emission characteristics: the radiative decay rate, quantum efficiency and angular emission. We use the model to study the continuous evolution of the antenna modes from perfectly-conducting antenna theory to quasi-static plasmonics.

We consider an elongated antenna of physical length L_p with a central section, of constant cross-sectional shape and size, that supports a charge density wave with wave vector:

$$k = k' + ik''. \tag{1}$$

The antenna is terminated at both ends, forming a resonator, which we model as a two-mirror cavity, Fig. 1(a). The model developed applies to any cross-sectional shape, assuming k is known.

The waves originate from a source at position a along the antenna axis. Figure 1 shows three different sources: an electric dipole, a magnetic dipole and a transmission line. The dipoles represent electronic dipolar transitions; transition rates are proportional to the emitted power. Electric and magnetic dipoles differ in the direction of the induced waves on opposite sides of the source. The transition rate for an electric (magnetic) dipole depends on the electric (magnetic) mode density, i.e. the magnitude of the impedance. The trans-

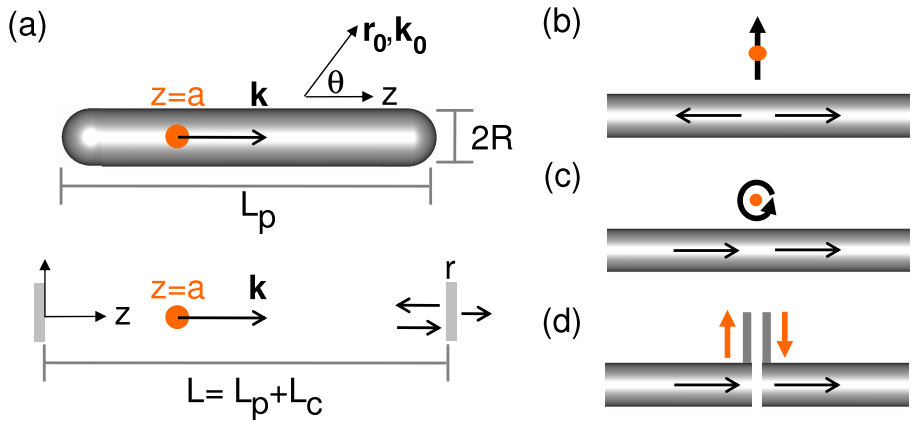


FIG. 1: (a) The antenna (total length L_p) is a rod of constant cross-sectional shape and size that supports a charge-density wave (wave vector k), and is terminated at both ends. It is driven by a local source at position $z = a$. We model the antenna as a 1D cavity with length L and amplitude reflection coefficient r. In a comparison with numerical calculations, we study cylindrical antennas with radius R and hemispherical ends. (b)-(d) Three local sources and the direction of the waves induced: (b) electric and (c) magnetic dipole, (d) transmission line

mission line resembles a magnetic dipole, but the fraction of the energy fed into the antenna is determined by impedance matching instead [20, 21, 22]. As a result, dipolar transitions dominantly excite different modes than standard center-fed antennas.

Resonant modes are expected for physical antenna lengths that are shifted from the multiples of π/k' by a constant value [7, 16, 19]. When modeling the antenna as a cavity, this displacement can be introduced by a positive phase shift upon reflection [12, 14, 16] or by an extended cavity length [19, 20]. The two corrections give the same resonant length, but are otherwise not equivalent. We choose to set an extended length $L = L_p + L_c$ and a real-valued reflection coefficient r.

To derive the resultant current distribution $I(z, a)$ we do not distinguish between conduction and displacement currents and assume a one-dimensional (1D) sinusoidal distribution. A superposition in complex notation for time-harmonic waves gives, for $0 \leqq z < a$,

$$I(z,a) = \frac{I_0(re^{ikz} - e^{-ikz})}{1 - r^2e^{2ikL}}(e^{ika} \pm re^{-ika}e^{2ikL}), \tag{2}$$

and, for $a < z \leqq L$,

$$I(z,a) = \frac{I_0(re^{ika} \pm e^{-ika})}{1 - r^2e^{2ikL}}(e^{ikz} - re^{-ikz}e^{2ikL}). \tag{3}$$

The initial amplitude of the induced wave I_0 depends on the type of dipole, its oscillator strength, and the three-dimensional (3D) configuration.

The + signs in equations 2 and 3 are for electric dipoles, the − signs for magnetic dipoles; electric and magnetic dipoles couple effectively to the antenna modes at different positions, a result of the geometrical argument in figure 1. The magnetic mode density maxima coincide with the electric mode density minima.

The diffracted far-field observed at r_0 is given by:

$$E_\theta = i\eta_0 \frac{k_0 e^{ik_0 r_0}}{4\pi r_0} \sin\theta \int_0^L I(z,a) e^{-ik_0 z\cos\theta} dz, \tag{4}$$

in which η_0 is the impedance and k_0 the wave vector for the surrounding medium. The other components of the electric field are zero. After evaluating the integral, equation 4 becomes:

$$E_\theta = \frac{iI_0E_0}{1-r^2e^{2ikL}}\Big[A\big(\frac{re^{-i(k_\parallel-k)a}-r}{k_\parallel-k} - \frac{e^{-i(k_\parallel+k)a}-1}{k_\parallel+k}\big)$$

$$+ B\big(\frac{e^{-i(k_\parallel-k)L}-e^{-i(k_\parallel-k)a}}{k_\parallel-k} - \frac{e^{-i(k_\parallel+k)L}-e^{-i(k_\parallel+k)a}}{r^{-1}e^{-2ikL}(k_\parallel+k)}\big)\Big], \tag{5}$$

in which, $k_\parallel = k_0\cos(\theta)$ is the projection of k_0 along the antenna axis, and $E_0 = i\eta_0 k_0 e^{ik_0r_0}\sin\theta/(4\pi r_0)$. $A = e^{ika} \pm re^{-ika}e^{2ikL}$ and $B = re^{ika} \pm e^{-ika}$ contain the dependence on the dipole position.

The angular emission in equation 5 is one of the main results of this letter. It gives a complete description of the interaction of the antenna with a dipole and with radiation. It describes the emission of the dipole through the antenna mode and, by reciprocity [9], its excitation by radiation.

Next, we use the derived model to study the main characteristics of optical antennas in a set of concrete examples, and compare the results to numerical simulations. We show how these characteristics evolve as the antenna modes become increasingly more bound, i.e. plasmonic. As a measure of how bound antenna modes are, we define an effective index K:

$$K \equiv k'/k_0. \tag{6}$$

As a concrete case we choose cylindrical gold antennas with hemispherical ends, Fig. 1(a). We study three radii, $R = 20, 10$ and 5 nm, which give different values for K [18, 19]. We vary the antenna length L for a constant wavelength. As a source, we choose an electric

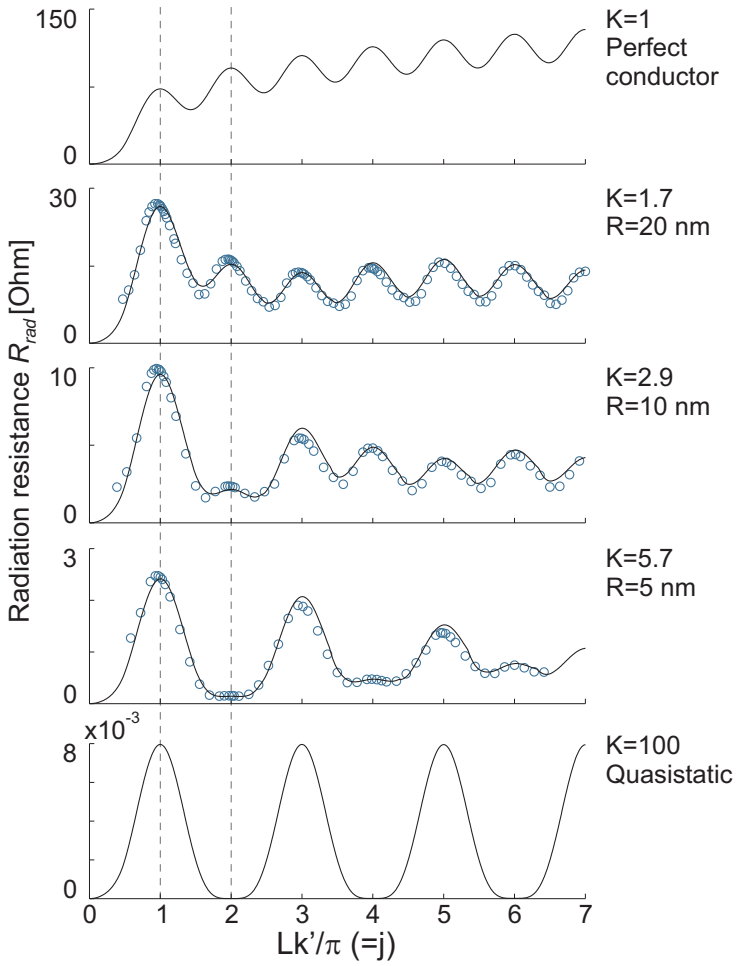


FIG. 2: Evolution of the radiation resistance $R_{rad}(L)$ for increasingly bound antennas, i.e. increasing K. The optical antennas ($K = 1.7, 2.9$ and 5.9) are intermediate cases between the limits of perfect electrical conductors ($K = 1$) and quasistatics ($K = 100 >> 1$). Resonant modes occur if $Lk'/\pi = j$, with j an integer. Lines: 1D model. Circles: 3D Numerical calculations for cylindrical gold antennas in vacuum (CST MicroWave Studio), Fig. 1. **Parameters** $\lambda_0 = 826.6$ nm. 3D Numerical: $\varepsilon_{au} = -29 + 2.0i$. Electric dipole at 5, 2.5 and 1.25 nm from the antenna end, placed on and oriented along the antenna axis. 1D model: Electric dipole at $a = 0$ and $r = 1$. For $K = 1$ and $K = 100$, $k'' = 0$. For $R = 20, 10$ and 5 nm: $k/k_0 = 1.7 + 0.048i, 2.9 + 0.11i$ and $5.7 + 0.26i$, and $L_c = 54, 26$ and 12 nm.

dipole at the antenna end, because it effectively excites all relevant resonant modes: $a = 0$ (L_c is added right of the dipole).

To study the radiation damping, we define a radiation resistance for $r = 1$ as:

$$R_{rad} \equiv 2P/I_{max}^2, \tag{7}$$

with P the total emitted power and I_{max} the maximum of $|I(z)|$ (Eqs. 2 and 3). The radiation resistance gives the radiation damping per unit amplitude in the resonator; it is independent of the total amplitude and is a characteristic of the spatial distribution of the mode.

The evolution of the radiation resistance with increasingly bound modes is illustrated in figure 2, which shows R_{rad} as a function of L for the three optical antennas, together with the limiting cases of $K = 1$ (thin perfectly-conducting antenna), and large K (quasi-static limit). We make the following four observations. First, the analytical results match the 3D numerical calculations. Second, the modes excited by electric dipoles at $a = 0$ differ from transmission-line center-fed antenna modes [23]. Magnetic dipoles at $a = L/2$ do reproduce the results for center-fed perfectly-conducting [23] ($K = 1$) and carbon nano-tube [22] ($K = 100$) antennas. Third, unlike for $K = 1$, the radiation resistance for optical antennas does not increase with increasing length; the waves are bound. Fourth, the radiation resistance decreases with increasingly bound modes, i.e. increasing K.

In the limit of $K >> 1$, equation 5 yields $R_{rad} \propto 1/K^2$, and since $K \propto 1/R$ [18], this also implies $R_{rad} \propto R^2$. The resonances are scale invariant only if $L_c \propto R$, or equivalently if the reflection phase is constant, which explains previous unexpected calculation results [17], and definitions [19].

We label the resonant modes $j = 1, 2...$ with $L = j\pi/k'$. Even and odd modes evolve differently; the radiation resistance of even modes diminishes with increasing K. These modes have anti-symmetric current distributions and no net dipole moment. For small antennas, i.e. $K >> 1$, these modes become subradient; the antenna modes scatter in all directions, opposite-oriented current elements cancel and the radiation resistance tends to zero. The nanorod antenna is not a simple Fabry-Pérot cavity. The dependence of the radiation resistance on the antenna length L implies that the reflection coefficient r is not a constant. We relate r to the radiation resistance:

$$r(L) = \frac{Z - R_{rad}/2}{Z + R_{rad}/2}, \tag{8}$$

in which Z is the real part of the antenna wave impedance, which is taken as a free parameter

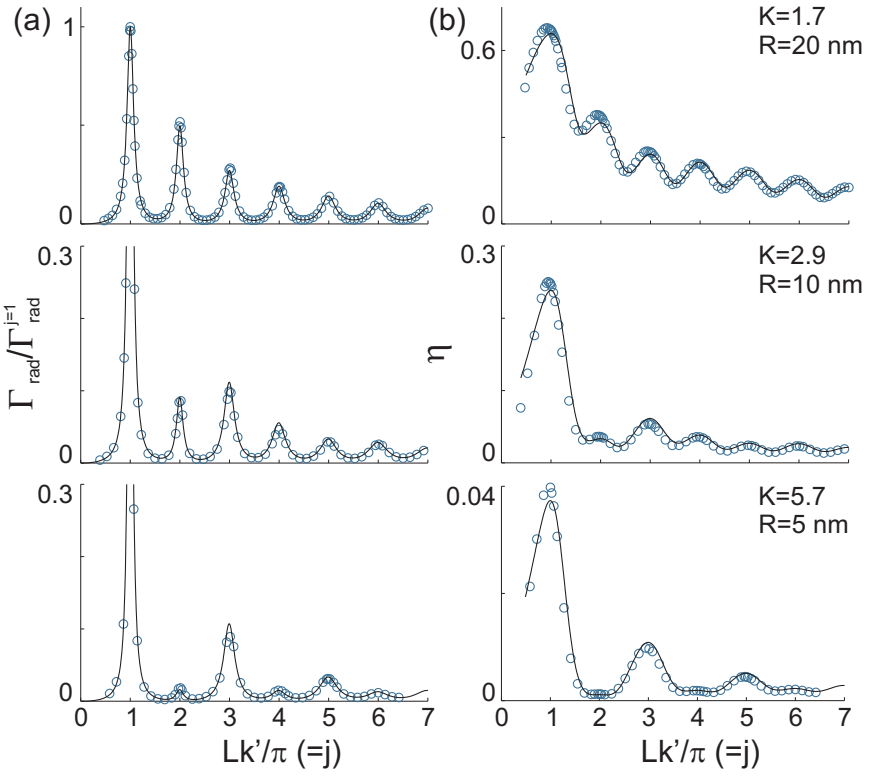


FIG. 3: The radiative transition rate Γ_{rad} relative to the rate for $j = 1$ (a) and the quantum efficiency η (b) for the three optical antennas. All parameters as in figure 2, but r from equation 8 with $Z = 165, 250$ and 450Ω.

here. Equation 8 is obtained by equating the reflection loss in the cavity model with the antenna radiation. It assumes: that all radiative loss is due to reflection, which is partly justified for bound waves; that the dissipation is small so that I_{max} is an approximate measure for the current at all positions; and that R_{rad} depends weakly on r.

With r defined, the radiative transition rate Γ_{rad} ($\propto P$) can be compared quantitatively for the different resonant modes, Fig. 3(a). The relative values for Γ_{rad} agree well with the numerical results. If r is taken constant instead, larger deviations are observed (e.g. for $R = 10$ nm, the error for the $j = 2$ peak is 8% for $r(L)$ and 18% for r constant). While for $K = 1$ all modes are pronounced, even modes disappear with increasing K. If the loss is dominated by dissipation, subradiant modes evolve into dark modes with small Γ_{rad}, despite the decreased damping due to low R_{rad}. By reciprocity, a small Γ_{rad} implies low field enhancements [9]; these dark modes interact weakly with radiation. For larger K, higher order modes are weaker compared to the $j = 1$ mode; for low R_{rad} the dissipative

losses (k'', per length) dominate the radiative losses (r, per reflection/roundtrip), and Γ_{rad} decays quickly with increasing L.

The balance between radiative and dissipative (Γ_{nr}) rates gives rise to a quantum efficiency $\eta = \Gamma_{rad}/(\Gamma_{rad} + \Gamma_{nr})$. The intrinsic efficiency of the dipole emitter is taken as unity. The constant additional dissipation due to the proximity of the dipole to the metal is not included in the model and is subtracted from the numerical results. Thus, η is the antenna efficiency and sets an upper limit to the quantum efficiency of emission through the antenna modes.

The efficiency generally decreases with K, particularly for the even modes, because the radiation resistance decreases, Fig. 3(b). Clearly, an efficient antenna should not be too plasmonic and should in general operate away from the quasi-static small-particle plasmon resonance. In applications where efficient conversion into a photon is not required, large-K subradiant modes with low radiation damping, and thus narrow line-widths, can be advantageous. Examples are sensors [24] and spasers [25].

The angular emission (Eq. 5) describes under which angles the antenna emits and can be effectively excited. Unlike previous 0D models [26], our model gives the emission patterns of higher order modes in good agreement with numerical calculations (Fig. 4). Even modes do not interact with radiation perpendicular to the antenna axis, as expected by symmetry arguments [15, 27]. The lossy nature of the modes introduces asymmetry, which reveals the position of the dipole. Higher order modes can give multi-lobed patterns with an odd or even amount of maxima for odd or even modes respectively. If $K >> 1$ then $k_\parallel \pm k \approx \pm k$, and the θ dependence of the denominator terms can be neglected. The emission is then a sum of three dipole terms: E_0, $E_0 e^{-ik_\parallel L}$ and $E_0 e^{-ik_\parallel a}$, with the latter contribution negligible for strong modes. The emission is given by two dipoles at the antenna ends, making a nanorod similar to a 2-slit configuration, and giving a basis for the intuitive picture of scattering of the mode at the antenna ends [11, 17, 28, 29].

We summarize the interaction of the modes with radiation in a phase-matching equation for nano-particles:

$$k_\parallel + (2m+1)k_L = k'. \tag{9}$$

In which $k_L = \pi/L$, and $m = 0, 1, 2...$ approximately give the maxima of interaction (Fig. 4). Modes that do not give solutions for equation 9 do not interact effectively with radiation

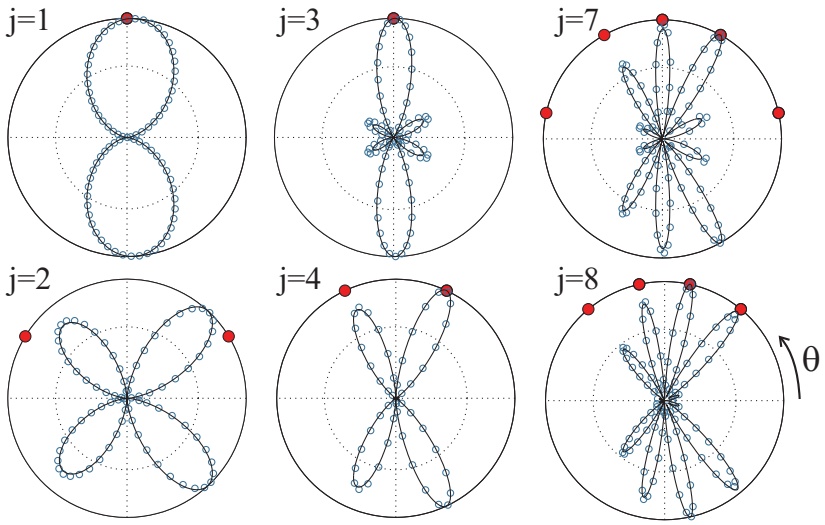


FIG. 4: Angular (θ) emitted power for modes j. $R = 20$ nm, all other parameters as in figure 3. 1D model: line. 3D numerical: circles (blue). Phase matching, Eq. 9: dots (red).

under any angle, and are subradiant/dark modes. Odd modes always give at least one solution, $m = (j-1)/2$. Even modes only yield solutions if $Lk_0 > \pi$, a condition depending only on L and k_0 as expected for a diffraction problem.

To conclude, the derived model accurately describes the interaction of dipolar emitters with radiation through nano-rod modes. The antenna properties are primarily governed by a single parameter $K = k'/k_0$ that describes how plasmonic the antenna modes are, and are summarized in a phase-matching equation. Although here we focused on the evolution of the emission properties for increasingly bound waves, the model applies to all interactions with any spatio-temporal beam and is equally valid for field enhancement and scattering problems. The results are thus widely applicable and might lead to further insights and design rules for optical antennas, nano-rod spasers [25], and generally for coupling light in/from nano-rods [11, 16, 17, 27, 28].

THT thanks R. Gordon for discussions.

[1] J.-J. Greffet, Science **308**, 1561 (2005)

[2] T. H. Taminiau et al., Nature Photon. **2**, 234 (2008)

[3] K. B. Crozier et al., J. Appl. Phys. **94**, 4632 (2003)

[4] P. Muhlschlegel et al., Science **308**, 1607 (2005)

[5] S. Kuhn et al., Phys. Rev. Lett. **97**, 017402 (2006)

[6] P. Anger, P. Bharadwaj, and L. Novotny, Phys. Rev. Lett. **96**, 113002 (2006)

[7] T. H. Taminiau et al., Nano Lett. **7**, 28 (2007)

[8] M. Ringler et al., Phys. Rev. Lett. **100**, 203002 (2008)

[9] T. H. Taminiau, F. D. Stefani, and N. F. van Hulst, Opt. Express **16**, 10858 (2008)

[10] G. W. Bryant, F. J. Garcia de Abajo, and J. Aizpurua, Nano Lett. **8**, 631 (2008)

[11] H. Ditlbacher et al., Phys. Rev. Lett. **95**, 257403 (2005)

[12] G. Della Valle, T. Sondergaard, and S. I. Bozhevolnyi, Opt. Express **16**, 6867 (2008)

[13] S. I. Bozhevolnyi and T. Sondergaard, Opt. Express **15**, 10869 (2007)

[14] E. S. Barnard et al., Opt. Express **16**, 16529 (2008)

[15] L. Douillard et al., Nano Lett. **8**, 935 (2008)

[16] J. Dorfmuller et al., Nano Lett. **9**, 2372 (2009)

[17] R. Kolesov et al., Nature Phys. **5**, 470 (2009)

[18] D. E. Chang et al., Phys. Rev. B **76**, 035420 (2007)

[19] L. Novotny, Phys. Rev. Lett. **98**, 266802 (2007)

[20] A. Alu and N. Engheta, Phys. Rev. Lett. **101**, 043901 (2008)

[21] A. Alu and N. Engheta, Nature Photon. **2**, 307 (2008)

[22] P. J. Burke, L. Shengdong, and Y. Zhen, IEEE Trans. Nanotechnol. **5**, 314 (2006)

[23] C. A. Balanis, *Antenna Theory: Analyses and Design*, 3rd ed. (John Wiley and Sons, Inc., Hoboken, New Jersey, 2005)

[24] F. Hao et al., Nano Letters **8**, 3983 (2008)

[25] D. J. Bergman and M. I. Stockman, Phys. Rev. Lett. **90**, 027402 (2003)

[26] E. R. Encina and E. A. Coronado, J. Phys. Chem. C **112**, 9586 (2008)

[27] G. Schider et al., Phys. Rev. B **68**, 155427 (2003)

[28] A. V. Akimov et al., Nature **450**, 402 (2007)

[29] P. Ghenuche et al., Phys. Rev. Lett. **101**, 116805 (2008)